Fibroblast Growth Factor 21-Deficient Mice Demonstrate Impaired Adaptation to Ketosis

Michael K. Badman, Anja Koester, Jeffrey S. Flier, Alexei Kharitonenkov, and Eleftheria Maratos-Flier

Division of Endocrinology, Diabetes, and Metabolism (M.K.B., J.S.F., E.M.-F.), Beth Israel Deaconess Medical Center, and Harvard Medical School (J.S.F.), Boston, Massachusetts 02215; and BioTechnology Discovery Research (A.Ko., A.Kh.), Lilly Research Laboratories, Indianapolis, Indiana 46285

Fibroblast growth factor 21 (FGF21) is a key metabolic regulator. Expressed primarily in liver and adipose tissue, FGF21 is induced via peroxisome proliferator-activated receptor (PPAR) pathways during states requiring increased fatty acid oxidation including fasting and consumption of a ketogenic diet. To test the hypothesis that FGF21 is a physiological regulator that plays a role in lipid oxidation, we generated mice with targeted disruption of the *Fgf21* locus (FGF21 knockout). Mice lacking FGF21 had mild weight gain and slightly impaired glucose homeostasis, indicating a role in long-term energy homeostasis. Furthermore, FGF21KO mice tolerated a 24-h fast, indicating that FGF21 is not essential in the early stages of starvation. In contrast to wild-type animals in which feeding KD leads to dramatic weight loss, FGF21KO mice fed KD gained weight, developed hepatosteatosis, and showed marked impairments in ketogenesis and glucose control. This confirms the physiological importance of FGF21 in the adaptation to KD feeding. At a molecular level, these effects were accompanied by lower levels of expression of PGC1α and PGC1β in FGF21KO mice, strongly implicating these key transcriptional regulators in the action of FGF21. Furthermore, within the liver, the maturation of the lipogenic transcription factor sterol regulatory element-binding protein-1c was increased in FGF21KO mice, implicating posttranscriptional events in the maladaptation of FGF21KO mice to KD. These data reinforce the role of FGF21 is a critical regulator of long-term energy balance and metabolism. Mice lacking FGF21 cannot respond appropriately to a ketogenic diet, resulting in an impaired ability to mobilize and utilize lipids. **(*Endocrinology* 150: 4931–4940, 2009)**

Fibroblast growth factor 21 (FGF21) is a member of the endocrine FGF subfamily (reviewed in Refs. 1 and 2), which also includes FGF23, human FGF19, and its mouse homolog FGF15. In mice, FGF21 is expressed predominantly in the liver (3). Pharmacologically, FGF21 induces glucose uptake through the induction of GLUT1 in adipocytes, and *in vivo* treatment with FGF21 results in amelioration of glucose and lipid parameters in both murine and nonhuman primate models of diabetes and obesity (4–7). Furthermore, mice overexpressing FGF21 are resistant to diet-induced obesity and exhibit improved glucose homeostasis (4).

Expression of hepatic FGF21 is induced in response to fasting and other ketotic states such as ketogenic diet (KD) feeding, primarily but not exclusively under the control of peroxisome proliferator-activated receptor-α (PPARα) (8–10). Furthermore, we have previously shown that in KD-fed mice, FGF21 plays a significant role in regulating lipid oxidation in the liver and adenoviral-mediated knockdown leads to hepatosteatosis and impaired ketosis (8).

FGF21 is also expressed in adipose tissue where mRNA levels are regulated by PPARγ (11, 12). The interplay between FGF21 and PPARγ is complex because treatment of adipocytes with FGF21 appears to increase PPARγ pro-

ISSN Print 0013-7227 ISSN Online 1945-7170
Printed in U.S.A.

doi: 10.1210/en.2009-0532 Received May 8, 2009. Accepted July 29, 2009.
First Published Online October 9, 2009

Abbreviations: BAT, Brown adipose tissue; CLAMS, comprehensive lab animal monitoring system; FGF21, fibroblast growth factor 21; FGF21KO, FGF21 knockout; KD, ketogenetic diet; PGWAT, perigonadal white adipose tissue; PPARα, peroxisome proliferator-activated receptor-α; PGC, PPAR-coactivator; qPCR, quantitative PCR; RER, respiratory exchange ratio; SREBP1, sterol regulatory element-binding protein-1; VO_2, oxygen consumption; VCO_2, carbon dioxide elimination; WT, wild type.

tein levels (11). Human studies show that increased circulating levels of FGF21 are found in obese individuals and subjects with metabolic syndrome or type 2 diabetes and suggest that in addition to liver, adipose tissue may be a potential physiological source of circulating FGF21 (13, 14).

At a cellular level, FGF21 interacts with an essential coreceptor βklotho and activates tissue-specific FGF receptors to activate MAPK and Akt pathways (4, 15–19). Although separate overexpression and adenoviral knockdown studies suggest FGF21 modulates a well defined program of gene expression (8, 9), the effector molecules downstream of MAPK and Akt responsible for these effects have yet to be elucidated.

Thus, it appears that FGF21 plays a critical role in various aspects of metabolism. To better understand the physiological role of endogenous FGF21 as a metabolic regulator, we generated mice with a targeted disruption of the *Fgf21* locus. At young ages, the phenotype of chow-fed FGF21 knockout (FGF21KO) mice was unremarkable. However, as these mice aged, they developed mild obesity and impaired glucose homeostasis. Furthermore, feeding of a KD revealed in full a dramatic phenotype of FGF21 deficiency. In contrast to normal animals, which become ketotic and lose substantial amounts of weight when fed this diet, FGF21KO mice had impaired ketosis and gained rather than lost weight. This was associated with altered gene expression both in the liver and adipose tissue. Our findings confirm FGF21 as a physiological regulator essential both for energy balance in the baseline state and for the adaptation to changes in dietary composition.

Materials and Methods

Generation of mice with targeted disruption of *Fgf21*

To generate mice with targeted disruption of the *Fgf21* locus, a 6.5-kb *Nhe*I genomic fragment containing all three exons of the mouse FGF21 gene was subcloned and used as a gene targeting vector by replacing part of exon 1 (30 bp downstream of the ATG), all of exon 2, and the 5′ region of exon 3 with a neomycin resistance gene (pGTN29; New England Biolabs, Ipswich, MA) thus deleting approximately 1200 bp of the genomic FGF21 sequence and deleting the 3′ part of exon 1, all of exon 2, and the 5′ region of exon 3. Founder mice were subsequently backcrossed onto the C57/BL6 line at least 10 times before investigation.

Mouse maintenance

All procedures were approved by the Beth Israel Deaconess Medical Center Institutional Animal Care and Use Committee. FGF21KO mice and wild-type (WT) littermates were maintained in a temperature-controlled environment at about 24 C under a 12-h light, 12-h dark cycle (0600–1800 h) with *ad libitum* access to food and water or water alone when fasted. Initially, mice were housed in groups of three to four, and during subsequent investigation, mice were housed singly with cage enrichment. Mice were fed either regular chow (Harlan Teklad F6 Rodent Diet; Madison, WI) or KD (Bio-Serv F-3666; Frenchtown, NJ) consisting of 78.9% fat, 9.5% protein, and 0.76% carbohydrate wt/wt) (20). Mice were euthanized between 0900 and 1100 h by lethal overdose of pentobarbital, exsanguinated, and rapidly dissected. Tissues were flash frozen and serum separated and frozen for further analysis. All experiments were performed using male mice in cohorts consisting of five to nine mice.

Indirect calorimetry

The metabolic rate of mice was measured at ambient temperature (~24 C) by indirect calorimetry of singly housed animals within open-circuit oxymax chambers of the comprehensive lab animal monitoring system (CLAMS; Columbus Instruments, Columbus, OH). Briefly, mice were acclimated to monitoring cages for 48 h before data acquisition (20–22). Mice were then placed in CLAMS chambers for up to 72 h during which time locomotor activity, oxygen consumption (VO_2) and carbon dioxide elimination (VCO_2) were monitored in real time. Respiratory exchange ratio (RER) and heat data were calculated using the equations RER = VCO_2/VO_2, and heat = $(3.815 + 1.232 \times \text{RER}) \times VO_2$.

Glucose homeostasis

Glucose homeostasis was assessed in FGF21KO and age-matched WT mice of 28–30 wk of age. Intraperitoneal glucose tolerance tests were performed at 0900 h on mice fasted 16 h using a One-Touch glucometer (Abbot Labs, Abbott Park, IL) to measure glucose blood sampled from tail vein after ip injection of 1 g/kg dextrose. Insulin tolerance tests were performed at 1400 h on mice fasted for 6 h in which glucose was measured using a One-Touch glucometer after ip injection of either 0.75 or 1 IU/kg regular insulin (Eli Lilly and Co., Indianapolis, IN).

Body composition analysis

Body composition was determined using an EchoMRI 3-in-1 quantitative nuclear magnetic resonance (qNMR) system (Echo Medical Systems, Houston, TX). Body fat, lean mass, body fluids, and total body water were measured between 1100 and 1300 h in live conscious mice with *ad libitum* access to chow or KD or after a 24-h fast. After euthanasia, mice were dissected, and the wet weight of whole liver, perigonadal fat pad, and total brown adipose tissue (BAT) depots were established.

Histological and ultrastructural analysis

Liver, perigonadal white adipose tissue (PGWAT) and BAT were fixed in 4% formal saline solution at 4 C overnight and processed for embedding in wax. Subsequent processing was performed by the histology core at Beth Israel Deaconess Medical Center. Five-micrometer sections were obtained and stained with hematoxylin and eosin and examined at ×40 magnification. Images of adipose tissue were analyzed to establish cell size by an investigator blinded to the experimental status of the sections involved. For this analysis, tissue from four mice from each group was examined; five distinct fields were visualized, and the diameter of five cells in each field was determined. For electron microscopic analysis, liver tissue was fixed in Karnovsky's solution and subsequently stained with osmium tetroxide and counterstained with uranyl acetate be-

fore embedding in epoxy resin. Ultrathin sections were then cut using a diamond knife, lead stained, and viewed under low and high magnification using a Tecnai G^2 Spirit BioTWIN transmission electron microscope.

Biochemical tissue analysis

Liver triglyceride was extracted by homogenization of 100 mg tissue in 1 ml extract buffer containing 0.1% Triton X-100 and subsequent incubation at 60 C for 1 h. Triglyceride content of unfractionated homogenate was determined using colorimetric assay (StanBio, Boerne, TX). Liver glycogen was assayed by homogenization of tissue samples in 0.5 N NaOH and subsequent ethanol precipitation of glycogen with Na_2SO_4 as a carrier. After resuspension and digestion of glycogen with α-amyloglucosidase for 1 h, liberated glucose concentration was measured in tissue samples and compared with that of bovine hepatic glycogen standard using calorimetric glucose assay (StanBio).

Serum analysis

After collection, serum was stored at −80 C before analysis. Glucose, β-hydroxybutyrate, triglycerides (StanBio) and nonesterified fatty acids (NEFAs) (Wako NEFA C; Wako Chemicals, Richmond, VA) were measured in duplicate using enzyme colorimetric assays. Insulin levels were determined by ultrasensitive mouse-specific ELISA (Crystal Chem, Downers Grove, IL). Leptin levels were determined in duplicate by mouse-specific ELISA (Crystal Chem) including a 1:10 dilution of serum of obese animals. FGF21 was measured in duplicate by RIA (Phoenix Pharmaceuticals, Burlingame, CA) with 100% cross-reactivity between human and rodent FGF21.

RNA extraction and quantitative real-time PCR

RNA was extracted with RNeasy tissue mini kit with on-column deoxyribonuclease digestion (QIAGEN, Valencia, CA). cDNA was synthesized from 1 μg total liver RNA with Ambion RETROscript (QIAGEN) using random decamer primers. Quantitative real-time PCR was performed in duplicate in a total reaction volume of 20 μl using SYBR-Green master mix (Applied Biosystems, Foster City, CA). Primers used were as previously published for metabolic and regulatory genes (8, 20), apart from primers recognizing sequences outside the targeting sequence of FGF21 forward CGTCTGCCTCAGAAGGACTC and reverse AAGGCTCTACCATGCTCAGG. Results are shown as relative expression in comparison with cyclophilin.

Immunoblot

Protein extracts in radioimmunoprecipitation assay (RIPA) buffer were mixed with SDS Laemmli loading buffer (Bio-Rad, Hercules, CA) containing 5% β-mercaptoethanol and heated for 10 min at 95 C. After resolving on 10% SDS-PAGE gels (Bio-Rad; Hercules, CA, proteins were transferred to Hybond-C extra nitrocellulose paper (Amersham, Piscataway, NJ), blocked with 5% milk, and then incubated with anti-sterol regulatory element-binding protein-1 (anti-SREBP1) antibody overnight at 4 C and horseradish peroxidase-conjugated antirabbit IgG, 1:5000 dilution, for 1 h at room temperature. Antibody binding was visualized by chemiluminescence (SuperSignal Substrate; Pierce Protein, Rockford, IL) and quantitation of exposed x-ray films performed with Image-J software (National Institutes of Health, Bethesda MD).

Statistical methods

All data are presented as mean ± SEM. Data sets were analyzed for statistical significance using a two-tailed unpaired Student's *t* test with StatView statistical software (SAS Institute Inc., Cary, NC). Statistical significance was assumed at $P < 0.05$.

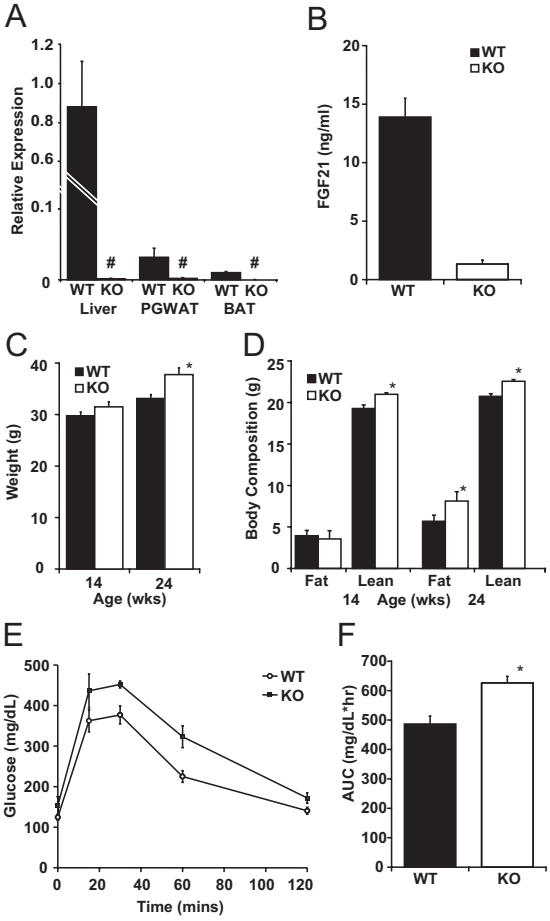

FIG. 1. Targeted disruption of the *Fgf21* gene produces mild obesity and glucose intolerance. A, Analysis of FGF21 expression by qPCR in liver, PGWAT, and BAT under KD-fed conditions reveals complete disruption of FGF21 expression (#, not detectable). B, Circulating serum FGF21 in KD-fed WT and FGF21KO (KO) mice shows negligible circulating FGF21immunoreactivity in mice with disrupted *Fgf21* allele. C, Weight of WT and FGF21KO mice at age 14 and 24 wk. A trend to greater weight in the FGF21KO mice was noted at 14 wk that became significant at 24 wk of age. D, Body composition of WT and FGF21KO mice at 14 and 24 wk as measured by quantitative nuclear magnetic resonance. Initially, FGF21KO mice had no difference in fat mass and a significant elevation in lean mass; by 24 wk, FGF21KO mice had significant increment in adipose depots with maintained increase in lean mass. E, Intraperitoneal glucose tolerance test in age-matched mice (WT 33.3 ± 0.8 g *vs.* FGF21KO 37.8 ± 1.3 g) showed no change in basal glucose but an increased glucose excursion in FGF21KO mice. F, Area under the curve (AUC) of glucose tolerance test was significantly elevated in FGF21KO mice. *, $P \leq 0.05$; *error bars* shown as SEM for groups of five to nine animals.

Results

Generation and validation of targeted disruption of *Fgf21* locus

The *Fgf21* locus was successfully disrupted by targeted insertion of a neomycin resistance cassette ablating exons 1 and 2 and the majority of exon 3. Because in chow-fed mice levels of FGF21 mRNA are very low, we used quantitative PCR (qPCR) to screen for FGF21 expression in tissues of WT and FGF21KO mice under conditions of KD feeding that leads to dramatic induction of FGF21. As we have previously reported, FGF21 mRNA was easily detectable in liver of WT mice fed KD and was also detected in PGWAT and BAT and as expected was below the limit of detection in FGF21KO mice across all tissues tested (Fig. 1A). In the KD-fed state, circulating FGF21 immunoreactivity, as measured by RIA, approached 15 ng/ml in WT mice but in FGF21KO mice was below the threshold for quantitation (Fig. 1B).

FGF21KO mice are prone to late-onset weight gain

When compared with WT littermates, FGF21KO mice were susceptible to late-onset weight gain when fed standard laboratory rodent diet. Body mass was mildly elevated after 14 wk, and this was significant at 24 wk of age (Fig. 1C). At 14 wk of age, body composition analysis revealed that the increase in mass was secondary to a small increase in lean weight (Fig. 1D). At 24 wk of age, FGF21KO mice accumulated more fat and body composition shifted so that both fat mass and lean mass were significantly elevated in FGF21KO mice in comparison with WT controls (Fig. 1D). Analysis of trunk and femur length showed no difference between WT and FGF21KO littermates. Increased body mass was associated with a moderate increase in daily caloric intake of chow by FGF21KO mice (16.7 ± 0.6 kcal/d WT *vs.* 21.4 ± 0.5 kcal/d FGF21KO). Notably, when corrected for body weight, this elevated caloric intake of chow remained significant (483 ± 18.5 kcal/kg · d WT *vs.* 562 ± 25 kcal/d FGF21KO).

FGF21KO mice have impaired glucose homeostasis

At 24 wk of age, glucose levels of FGF21KO and WT mice were similar whether animals were fed or fasted overnight or for 24 h (Table 1 and Fig. 1E). FGF21KO mice had a markedly increased glucose excursion in response to an ip glucose load (Fig. 1E) with significant increases in area under the curve (Fig. 1F). However, there was no difference in the response to ip insulin tolerance test performed in age-matched mice, despite an approximate 5 g difference in body weight (WT 33.8 ± 0.7 g *vs.* FGF21KO 39.0 ± 1.5 g) with either 1 U/kg or 0.75 U/kg insulin (data not shown).

TABLE 1. Circulating metabolites and hormones as measured in WT and FGF21KO mice fed, fasted, and after equilibration to KD feeding

Metabolite	Chow-fed		Fasted		KD-fed	
	WT	KO	WT	KO	WT	KO
Glucose (mg/dl)	180 ± 9.7^{c,d,e}	193 ± 10.1^{c,d,e,f}	72.1 ± 6.4^{e,f}	71.5 ± 14.3^{a,b,e,f}	131 ± 4.9^{a,b,c,d,f}	164 ± 8.0^{b,c,d,e}
β-Hydroxybutyrate (mmol/liter)	0.20 ± 0.03^{c,d,e,f}	0.20 ± 0.02^{c,d,e,f}	1.29 ± 0.09^{a,b,e,f}	1.39 ± 0.07^{a,b,e,f}	0.81 ± 0.13^{a,b,c,d,f}	0.50 ± 0.06^{a,b,c,d,e}
Triglycerides (mg/dl)	101 ± 12^{c,e}	104 ± 13^{c,d}	57 ± 6^{a,b,e}	72 ± 13^{e}	36.6 ± 5.4^{a,b,c,d,f}	74.1 ± 13.6^{e}
NEFA (mEq/liter)	0.69 ± 0.08^{c,d,e}	0.77 ± 0.08^{c,e,f}	1.21 ± 0.07^{a,b,d,e,f}	0.95 ± 0.05^{a,c,e,f}	0.46 ± 0.03^{a,b,c,d}	0.51 ± 0.05^{a,b,d}
Cholesterol (mg/dl)	ND	ND	ND	ND	94.2 ± 3.5^{f}	146 ± 13.8^{e}
Insulin (ng/ml)	ND	ND	0.54 ± 0.10^{e,f}	0.87 ± 0.21^{e,f}	1.98 ± 0.29^{c,d,f}	3.37 ± 0.44^{c,d,e}
Leptin (ng/ml)	ND	ND	ND	ND	1.5 ± 0.3^{f}	13.8 ± 2.0^{e}
Glucagon (pg/ml)	ND	ND	ND	ND	59.7 ± 3.3	55.7 ± 18

ND, Test not done.

Statistically significant differences ($P < 0.05$ *by t* test) are denoted as follows: [a] *vs.* chow-fed WT; [b] *vs.* chow-fed FGF21KO (KO); [c] *vs.* fasted WT; [d] *vs.* fasted KO; [e] *vs.* KD-fed WT; [f] *vs.* KD-fed (KO).

FGF21KO mice tolerate acute fasting

Fasting for 24 h from 2 h after lights on led to weight loss in both WT and FGF21KO mice, although the amount of weight lost by FGF21KO mice was less (Fig. 2A). After a 24-h fast, there was no difference in circulating glucose levels, ketones, or plasma triglyceride or NEFA concentrations (Table 1). There was no difference in physical activity between WT or FGF21 mice whether fed or fasted (Fig. 2B), nor was there any alteration in diurnal rhythmicity of ambulation (data not shown). In the chow-fed state, VO_2 was lower in FGF21KO compared with WT mice (Fig. 2C). During a 24-h fast, both WT and FGF21KO mice exhibited reduced VO_2 (Fig. 2C). Moreover, these changes were also apparent without correction for weight and were paralleled by calculated heat production (supplemental Fig. 1, A–D, published as supplemental data on The Endocrine Society's Journals Online web site at http://endo.endojournals.org). In *ad libitum* chow-fed mice, there was an appropriate reduction in RER during the light phase consistent with a shift from carbohydrate to fatty acid utilization in both WT and FGF21KO mice. In mice fasted for 24 h, there was a further reduction of RER in both WT and FGF21KO mice, and as expected, there was no diurnal variation (Fig. 2D). Core temperature did not differ between WT and FGF21KO mice under either chow-fed or fasting conditions (Fig. 2E).

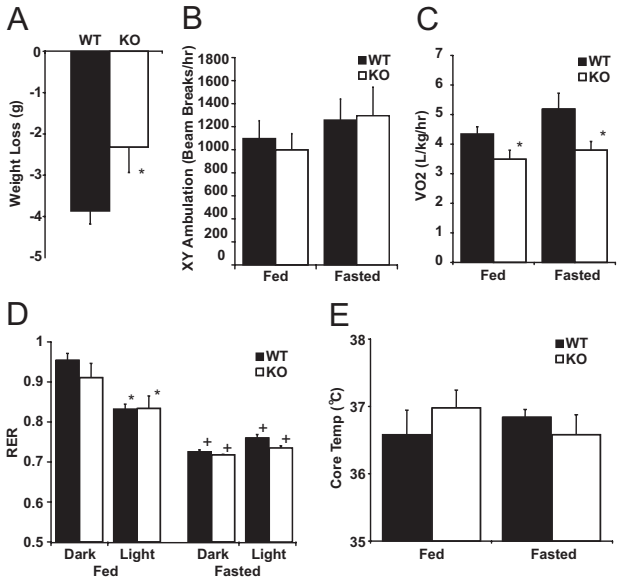

FIG. 2. Response of FGF21KO (KO) mice to 24 h of fasting. A, Total weight loss after a 24-h fast in CLAMS apparatus was significantly less in FGF21KO mice. B, Activity monitoring showed no difference in total 24-h ambulation between WT and FGF21KO mice in either fed or fasted conditions. C, Measurement in CLAMS apparatus showed significant decreases in VO_2 in FGF21KO mice in both fed and fasted conditions. D, Calculation of RER revealed significant reduction during light phase under fed conditions (*) and in both dark and light phases under fasted conditions (+). There was no difference between response of WT or FGF21KO was detected in either dark or light phases. E, Monitoring core temperature revealed no statistically significant change in core temperature in FGF21KO mice in either fed or fasted states. *, $P \leq 0.05$; *error bars* shown as SEM for groups of five to nine animals.

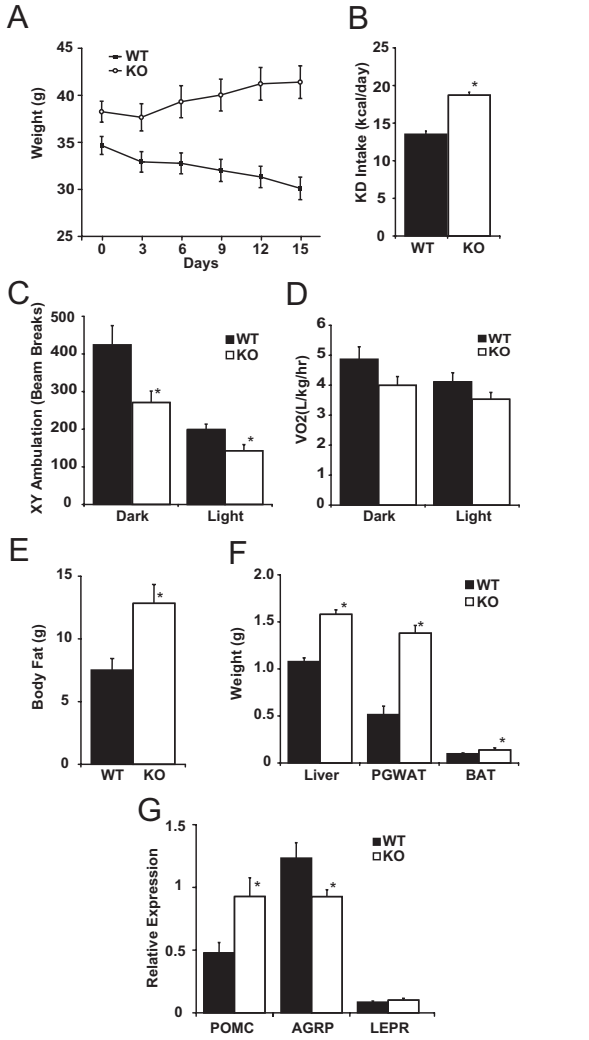

FIG. 3. Response of FGF21KO (KO) mice to KD feeding. A, Body weight of WT and FGF21KO mice switched from chow feeding (Day 0) to KD feeding showed increased body weight in FGF21KO mice in contrast to normal weight loss seen in WT mice. B, Mean caloric intake of KD-fed mice over 14 d of KD feeding showed increased consumption of KD in FGF21KO mice. C, Activity monitoring showed significant reduction in ambulation in FGF21KO mice in both dark and light phases. D, Measurement in CLAMS apparatus showed a trend toward reduced VO_2 in KD-fed FGF21KO mice however this difference failed to reach statistical significance in either dark or light phases. E, Body composition analysis of WT and FGF21KO mice fed KD for 14 d revealed significant increases in body fat in FGF21KO mice. F, Postmortem organ weights from WT and FGF21KO mice revealed increases in liver, PGWAT and BAT weights in FGF21KO mice. G, Analysis of hypothalamic neuropeptide expression by qPCR revealed induction of pro-opiomelanocortin (POMC) and suppression of agouti-related peptide (AgRP) mRNA. There was no difference in expression of leptin receptor (LEPR). *, $P \leq 0.05$; *error bars* shown as SEM for groups of five to nine animals.

FGF21KO mice fed KD gain weight

FGF21KO mice placed on a KD for 2 wk gained substantial weight (Fig. 3A) in distinct contrast to weight loss

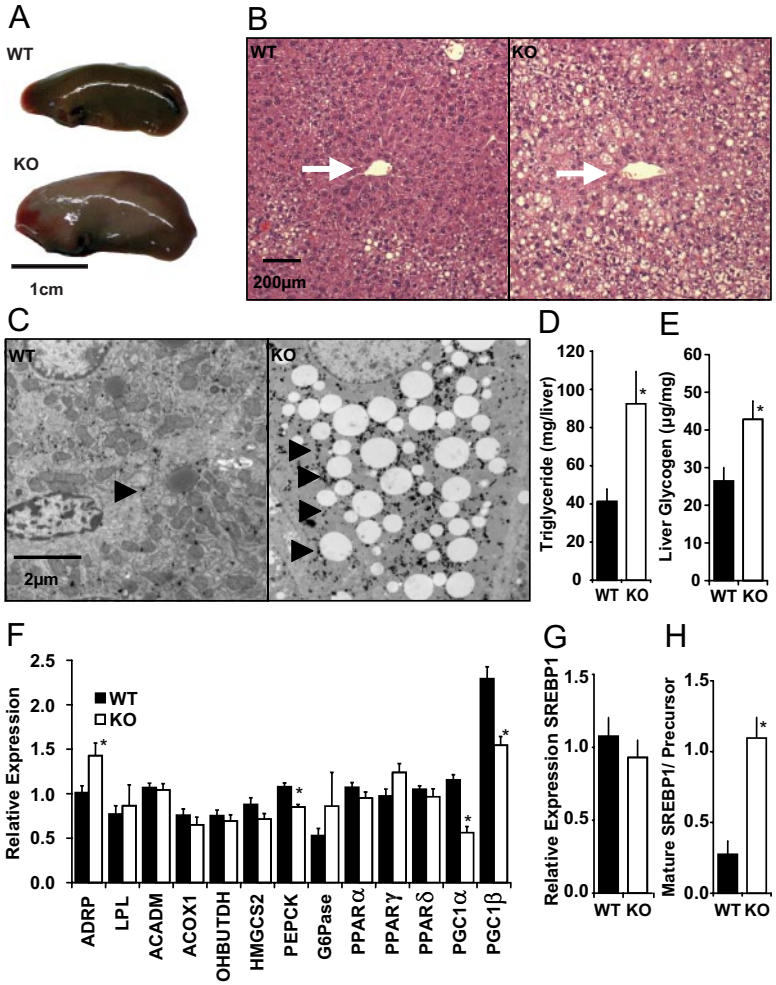

FIG. 4. FGF21KO mice are susceptible to hepatosteatosis and maladaptive changes in gene expression when fed KD. A, Macroscopically, FGF21KO (KO) mice had enlarged livers (left lobe only shown) with an increased fatty appearance. *Scale bar*, 1 cm. B, Light microscopy demonstrated the increased fatty appearance of liver in KD-fed FGF21KO mice. Increased fatty infiltration was noted at the periphery of the lobule in KD-fed WT mice; however fatty infiltration had a more marked centripetal spread toward the central vein (*white arrows*) in FGF21KO mice. *Scale bar*, 200 μm. C, Electron microscopy of hepatic cells midway between central vein and portal triad revealed marked fatty infiltration in FGF21KO mice and also increased staining of α-glycogen granules within the cytoplasm of FGF21KO hepatocytes (*arrow heads*). D, Biochemical determination of total triglyceride content of WT and FGF21KO mice livers revealed significantly elevated hepatic stores. E, Biochemical assay of glycogen showed significant increases in hepatic glycogen stores in FGF21KO mice. F, qPCR analysis of hepatic metabolic genes showed significant increases in adipose differentiation-related peptide (ADRP) in FGF21KO mice. There was a trend to decreased expression of ACADM, ACOX1, OHBUTDH and HMGCS2 that did not reach significance. PEPCK was significantly reduced in FGF21KO mice in the absence of regulation of G6Pase. There was no significant change in any PPAR isoform analyzed, yet PGC1α and PGC1β were significantly down regulated in FGF21KO mice. G, qPCR analysis revealed no significant change in SREBP1 expression at mRNA level. H, Immunoblot analysis revealed a significant shift from precursor to mature form of SREBP1. *, $P \leq 0.05$; *error bars* shown as SEM for groups of five to nine animals.

typical of WT mice (20). Compared with WT mice, FGF21 mice had a greater caloric intake (Fig. 3B) and had lower physical activity (Fig. 3C). VO_2 also trended lower in KD-fed FGF21KO mice (Fig. 3D). KD-fed FGF21KO mice had higher leptin, insulin, and glucose levels than WT mice (Table 1). The decrease in glucose levels from chow-fed baseline was less pronounced, and insulin levels were significantly higher in KD-fed FGF21KO compared with WT mice (Table 1). In FGF21KO mice, ketosis was impaired as demonstrated by lower β-hydroxybutyrate levels despite availability of substrates in the form of circulating NEFA, and triglycerides were higher in FGF21KO compared with WT mice (Table 1). Longitudinal analysis of body composition revealed a marked increase in body fat content (Fig. 3E). The changes in body composition were paralleled by significant elevation of liver, PGWAT, and BAT weights in FGF21KO mice compared with WT mice (Fig. 3F). Analysis of hypothalamic neuropeptides revealed higher expression of proopiomelanocortin (POMC) and lower expression of agouti-related peptide (AgRP) mRNA (Fig. 3G), findings consistent with increased circulating leptin levels in obese FGF21KO mice.

FGF21KO mice have fatty liver and altered hepatic gene expression

Consistent with increased hepatic weight, the livers of KD-fed FGF21KO mice were enlarged and grossly fatty in appearance (Fig. 4A). This fatty appearance was reflected at a histological level with lipid accumulation encroaching across the hepatic lobule toward the central vein (Fig. 4B). Electron-microscopic analysis of cellular ultrastructure revealed that, in addition to lipid accumulation, hepatocytes of FGF21KO mice were also laden with large numbers of α-glycogen granules (Fig. 4C). Biochemical analysis revealed that when fed KD, FGF21KO mice had 2-fold more hepatic triglyceride content (Fig. 4D) and a significant increase in liver glycogen (Fig. 4E) compared with WT littermates.

Gene expression analysis revealed an increase in adipose differentiation-related peptide (ADRP) consistent with increased fatty accumulation within the liver. There were relatively minor changes in expression of metabolic genes tested. Expression of acyl coenzyme A dehydrogenase medium chain (ACADM), acyl-coenzyme A oxidase 1 (ACOX1), 3-hydroxybutyrate dehydrogenase (OHBUTDH), and 3-hydroxy-3-methylglutaryl-coenzyme A synthase 2 (HMGCS2) all trended lower in FGF21KO mice (Fig. 4F). There was a significantly lower expression of phosphoenolpyruvate

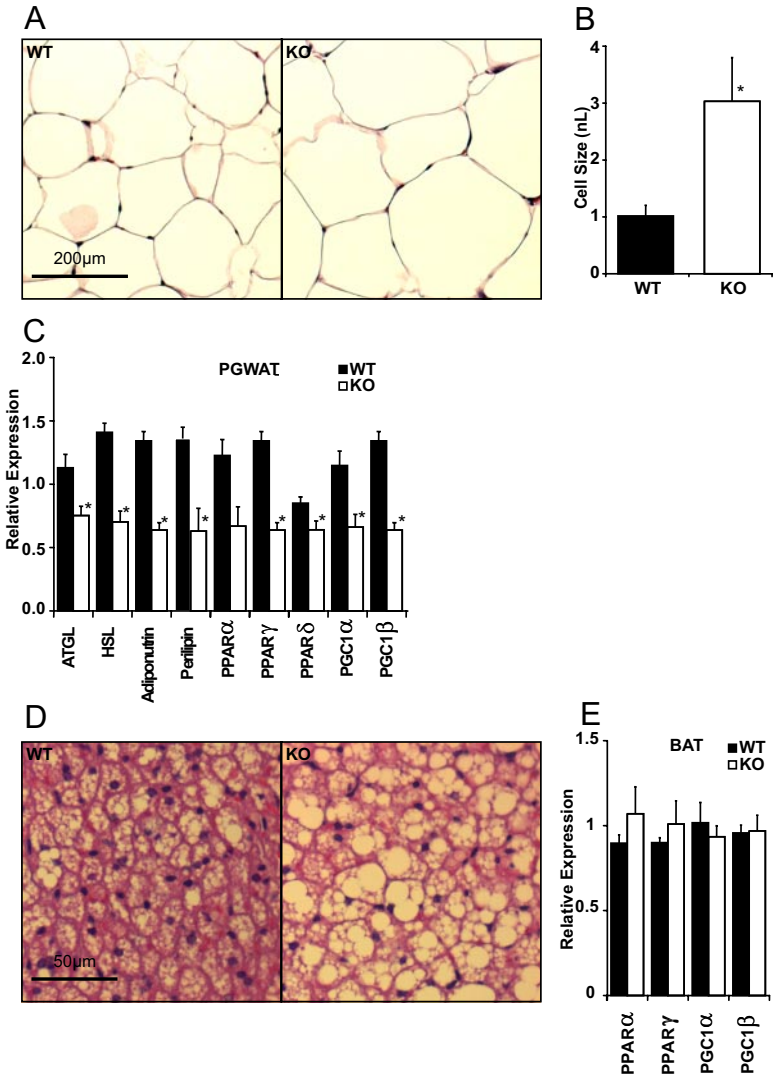

FIG. 5. FGF21KO (KO) mice develop white adipocyte hypertrophy when fed KD associated with decreased lipolytic and regulatory gene expression. A, Light microscopy showed increased adipocyte size in PGWAT depots of FGF21KO mice. *Scale bar*, 200 μm. B, Image analysis revealed a statistically significant increase in PGWAT cell volume in KD-fed FGF21KO, which was almost 3-fold that of WT mice. C, Gene expression analysis of PGWAT by qPCR showed a significant reduction in expression of lipases adipose triglyceride lipase (ATGL), hormone-sensitive lipase (HSL) and also adiponutrin in FGF21KO mice. There was a significant reduction in all PPAR isoforms investigated and a concomitant reduction in PGWAT expression of PGC1α and PGC1β in KD-fed FGF21KO compared with WT mice. D, Light microscopy showed increased fatty appearance of BAT. *Scale bar*, 50 μm. E, Gene expression analysis of BAT transcripts revealed no significant change in PPARα or γ or PGC1 isoforms. *, $P \leq 0.05$; *error bars* shown as SEM for groups of five to nine animals.

carboxykinase (PEPCK) but no difference in glucose-6-phosphatase (G6Pase) in FGF21KO mice compared with WT mice. No differences in expression of lipogenic genes fatty acid synthase (FAS) and stearoyl-coenzyme A desaturase 1 (SCD1) were found between KD-fed WT and FGF21KO mice (data not shown). Notably, in the absence of any changes in PPARα, -δ, or -γ expression of the PPAR-coactivators (PGC)-1α and PGC1β was markedly lower in FGF21KO mice compared with WT mice (Fig. 4F). In addition, although hepatic mRNA levels of SREBP1 were not significantly altered in FGF21KO mice (Fig. 4G), a marked increase in activation of SREBP1 at a posttranscriptional level was apparent with a significant increase in the ratio of mature SREBP1 to precursor (Fig. 4H).

FGF21KO mice exhibit abnormal expression of genes regulating lipid homeostasis in adipose tissue

Histological analysis revealed that the average size of adipocytes within PGWAT depots of FGF21KO mice were larger than those of WT mice (Fig. 5, A and B). Histological examination also revealed increased lipid stores in BAT (Fig. 5C). Gene expression analysis revealed marked reduction in mRNA of the lipolytic enzymes adipose triglyceride lipase (ATGL) and hormone-sensitive lipase (HSL) together with down-regulation of adiponutrin in FGF21KO mice compared with WT mice. These changes were paralleled by a reduction in expression of perilipin mRNA (Fig. 5D). Notably, there was reduced adipose expression of PPARα, -δ, and -γ and their coactivators PGC1α and PGC1β in the FGF21KO mice (Fig. 5D). In contrast, gene expression analysis revealed no significant changes in these regulators in the BAT of FGF21KO mice (Fig. 5E).

Discussion

The liver plays a critical role in mediating physiological adaptation from the fed to the fasted state. As nutrients from ingested food become unavailable, the liver provides glucose initially through glycogen breakdown. As fasting progresses, metabolic substrates stored in adipose tissue are released into the circulation as glycerol and free fatty acids. The liver then uses glycerol for *de novo* glucose synthesis and converts available lipids into ketone bodies. A number of hormones are known to play a role in this process, including insulin and glucagon. Recently, FGF21 has been added to the list of factors that regulate the response to fasting. Interestingly, consumption of very-high-fat, low-carbohydrate KD requires adaptations similar to fasting with regard to lipid oxidation, and FGF21 also plays a critical role in ketogenesis and lipid oxidation during consumption of these diets.

FGF21 is expressed predominantly in the liver where it is primarily regulated by PPARα (8–10); FGF21 is also

expressed in adipose tissue where it is potentially regulated by PPARγ (11, 23). Exogenous FGF21 treatment has been shown to cause weight loss and improve glucose homeostasis in rodent and primate models of metabolic disease (4, 5). More recently, FGF21 has been shown efficacious for weight loss and amelioration of fatty liver in diet-induced and genetic models of obesity (6, 7). We have previously demonstrated in mice fed a KD that adenovirally mediated knockdown of hepatic FGF21 leads to fatty liver, lipemia, and reduced circulating ketones (8). However, such knockdown studies are spatially and temporally constrained by tissue selectivity and immune response to viral vectors that, coupled with viremia-induced anorexia, makes this loss of function paradigm unsuitable for investigation of long-term effects on energy homeostasis. Therefore, to further understand the role of FGF21 in metabolism, we examined mice with global FGF21 deficiency.

Initial studies revealed no metabolic phenotype in young chow-fed FGF21KO mice. However, by the age of 14 wk, FGF21KO mice had a small increase in lean body mass, and mice aged beyond 24 wk developed mild obesity. This is in direct contrast to the phenotype of transgenic mice overexpressing FGF21 that are lean and resist diet-induced obesity (4, 9). Adiposity in FGF21KO mice was associated with both higher caloric intake and lower VO_2 in comparison with WT mice. Another notable feature of mice lacking FGF21 was mild glucose intolerance in the absence of a significant change in insulin sensitivity. This is consistent with the reports that exogenous FGF21 improves glucose homeostasis in obese animal models of diabetes (4–7).

When fasted for 24 h, FGF21KO mice lost less weight than WT littermates, suggesting that mobilization of energy stores is less effective in FGF21KO mice. This is consistent with the action of FGF21 to maintain nutrient flow from adipose stores to circulating lipid and ketone fuels in the fasted state (8, 9). The role of FGF21 in utilization of lipid stored is further supported by the finding that FGF21-overexpressing mice have decreased adipose energy stores (4, 9). In one report, mice overexpressing FGF21 were found to be prone to torpor (9). However, this has not been observed in analysis of separately derived mouse lines (24) or in long-term infusion studies in obese mice, so it is possible that the observed torpor is due to decreased availability of lipid fuels during fasting secondary to leanness. Because FGF21KO mice are potentially less able to mobilize peripheral fat stores, we were keen to assess the defense of core temperature during fasting. Notably, there was no change in core body temperature after a 24-h fast, and FGF21KO mice were free of calorimetric, ambulatory, or behavioral signs of torpor at this time point.

KD feeding leads to weight loss in WT mice and correction of metabolic status in WT mice subjected to diet-induced obesity (20). Feeding KD is associated with activation of hepatic PPARα, which leads to induction of FGF21 (8). Thus, it was of particular interest that disruption of the *Fgf21* locus not only prevented weight loss on KD but also led to marked accumulation of adipose tissue and maintained an elevated caloric intake in KD-fed FGF21KO mice. Gene expression profiles of hypothalamic neuropeptides suggested that the small increase in food intake and body weight was not centrally mediated. Suppressed hypothalamic levels of agouti-related peptide and increased neuropeptide Y compared with WT mice were consistent with high leptin levels noted in FGF21KO mice. Although unexplained, the mild hyperphagia seen in FGF21KO mice contrasts with increases in caloric intake that occur in FGF21-overexpressing mice in which increased feeding is likely to represent a compensation for increased energy utilization (4, 5).

The accumulation of fat in the liver is consistent with impaired ability of the liver to oxidize fatty acids in the absence of FGF21. Although a degree of hepatosteatosis occurs with KD feeding (20), the fatty accumulation is predominantly in a microvesicular pattern located at the periphery of the hepatic lobule (Kennedy, A. R., unpublished observations). In the absence of FGF21, KD feeding caused substantially more accumulation of hepatic fat, in a pattern wherein microvesicles extended to centrilobular regions. Of note, increases in hepatic triglyceride were paralleled by increased glycogen content in the absence of changes in expression of genes responsible for glycogen synthesis.

The mechanism by which FGF21 activates specific programs of gene expression suggested by both gain- and loss-of-function studies (8, 9) has not been fully explained. In the KD-fed state, FGF21KO mice exhibited much lower hepatic expression of PGC1α and PGC1β compared with WT littermates, which suggests that these coactivators are downstream of FGF21 action. This is consistent with our finding that adenoviral-mediated hepatic FGF21 knockdown produced a substantial reduction in expression of both PGC1α and PGC1β (supplemental Fig. 1, E and F).

Within the liver, FGF21 ablation appears to affect the maturation of SREBP1, a lipogenic transcription factor implicated in development of hepatosteatosis (25–28). We show that in FGF21KO mice, there is a marked increase in the maturation of SREBP1 in the absence of increases in SREBP1 mRNA or precursor protein levels. This mirrors the recent finding that pharmacological doses of FGF21 can reverse the increase in hepatic SREBP1 maturation

brought about by feeding a high-fat high-sucrose diet to WT mice (7). Elucidation of the mechanism by which FGF21 impacts on SREBP1 maturation will provide scope for further research.

Perhaps as a direct consequence of their impaired ability to use lipid fuels, mice lacking FGF21 showed increased fat stores when fed KD. Adipose depots of KD-fed FGF21KO mice were expanded in size due to hypertrophy of adipocytes. This mirrors findings in FGF21-overexpressing mice that have decreased adipocyte size (4, 9). Furthermore, PGWAT expression of ATGL and HSL were both reduced in FGF21KO mice compared with WT animals. Expression of these enzymes, responsible for triglyceride and diglyceride lipolysis, respectively, is modulated by PPAR activation and is induced at the RNA level in the adipose depots of FGF21-overexpressing mice (9). Although lipolysis is also regulated at a number of post-transcriptional levels, reduced gene expression is likely to impact on lipolytic potential. FGF21KO animals also showed an increase in lipid content in BAT tissue, consistent with an overall increased adiposity.

We have determined that FGF21KO mice are susceptible to late-onset adiposity and disturbed glucose handling that is consistent with the metabolic effect of pharmacological FGF21 administration. Although FGF21KO mice show only mild metabolic differences compared with WT mice during fasting, they have markedly atypical responses to feeding of a KD. Instead of weight loss seen in normal mice, there was substantial weight gain and exaggerated accumulation of fat in liver. These data further confirm the crucial metabolic role of FGF21 in systemic physiology of energy balance and metabolism, particularly in states such as fasting and consumption of a KD that require active hepatic lipid oxidation.

Acknowledgments

We are grateful for the help and advice of Maria Ericsson and Louise Trakimas of the Harvard Medical School EM facility and the expert technical assistance of Patrick Antonellis, Katherine Kurgansky, Fen Fen Liu, and Frank Marino in the production of this paper.

Address all correspondence and requests for reprints to: Eleftheria Maratos-Flier M.D., Associate Professor of Medicine, Division of Endocrinology, Diabetes, and Metabolism, Beth Israel Deaconess Medical Center, Center for Life Sciences, 7th Floor, 330 Brookline Avenue, Boston, Massachusetts 02215. E-mail: emaratos@bidmc.harvard.edu.

This work was supported by grants from the Picower Foundation (E.M.-F.), National Institutes of Health Grant R01 DK069983 and DK056116 (E.M.-F.), Grant R37 DK28082 (J.S.F.), and Boston Obesity and Nutrition Research Council Pilot and Feasibility Grant DK46200–15 (M.K.B.). Indirect calorimetry performed by the Beth Israel Deaconess Medical Center Animal Physiology Core was supported by National Institutes of Health Grant P01 DK56116.

Disclosure Summary: M.K.B. and J.S.F. have nothing to declare. A.Ko and A.Kh are employed by Lilly and Co. E.M.-F. has consulted for Lilly and Co. regarding FGF21.

References

1. **Moore DD** 2007 Physiology. Sister act. Science 316:1436–1438
2. **Kurosu H, Kuro-O M** 2009 The Klotho gene family as a regulator of endocrine fibroblast growth factors. Mol Cell Endocrinol 299: 72–78
3. **Nishimura T, Nakatake Y, Konishi M, Itoh N** 2000 Identification of a novel FGF, FGF-21, preferentially expressed in the liver. Biochim Biophys Acta 1492:203–206
4. **Kharitonenkov A, Shiyanova TL, Koester A, Ford AM, Micanovic R, Galbreath EJ, Sandusky GE, Hammond LJ, Moyers JS, Owens RA, Gromada J, Brozinick JT, Hawkins ED, Wroblewski VJ, Li DS, Mehrbod F, Jaskunas SR, Shanafelt AB** 2005 FGF-21 as a novel metabolic regulator. J Clin Invest 115:1627–1635
5. **Kharitonenkov A, Wroblewski VJ, Koester A, Chen YF, Clutinger CK, Tigno XT, Hansen BC, Shanafelt AB, Etgen GJ** 2007 The metabolic state of diabetic monkeys is regulated by fibroblast growth factor-21. Endocrinology 148:774–781
6. **Coskun T, Bina HA, Schneider MA, Dunbar JD, Hu CC, Chen Y, Moller DE, Kharitonenkov A** 2008 Fibroblast growth factor 21 corrects obesity in mice. Endocrinology 149:6018–6027
7. **Xu J, Lloyd DJ, Hale C, Stanislaus S, Chen M, Sivits G, Vonderfecht S, Hecht R, Li YS, Lindberg RA, Chen JL, Jung DY, Zhang Z, Ko HJ, Kim JK, Véniant MM** 2009 Fibroblast growth factor 21 reverses hepatic steatosis, increases energy expenditure, and improves insulin sensitivity in diet-induced obese mice. Diabetes 58:250–259
8. **Badman MK, Pissios P, Kennedy AR, Koukos G, Flier JS, Maratos-Flier E** 2007 Hepatic fibroblast growth factor 21 is regulated by PPARα and is a key mediator of hepatic lipid metabolism in ketotic states. Cell Metab 5:426–437
9. **Inagaki T, Dutchak P, Zhao G, Ding X, Gautron L, Parameswara V, Li Y, Goetz R, Mohammadi M, Esser V, Elmquist JK, Gerard RD, Burgess SC, Hammer RE, Mangelsdorf DJ, Kliewer SA** 2007 Endocrine regulation of the fasting response by PPARα-mediated induction of fibroblast growth factor 21. Cell Metab 5:415–425
10. **Lundåsen T, Hunt MC, Nilsson LM, Sanyal S, Angelin B, Alexson SE, Rudling M** 2007 PPARα is a key regulator of hepatic FGF21. Biochem Biophys Res Commun 360:437–440
11. **Moyers JS, Shiyanova TL, Mehrbod F, Dunbar JD, Noblitt TW, Otto KA, Reifel-Miller A, Kharitonenkov A** 2007 Molecular determinants of FGF-21 activity-synergy and cross-talk with PPARγ signaling. J Cell Physiol 210:1–6
12. **Muise ES, Azzolina B, Kuo DW, El Sherbeini M, Tan Y, Yuan X, Mu J, Thompson JR, Berger JP, Wong KK** 2008 Adipose fibroblast growth factor 21 is up-regulated by PPARγ and altered metabolic states. Mol Pharmacol 74:403–412
13. **Chen WW, Li L, Yang GY, Li K, Qi XY, Zhu W, Tang Y, Liu H, Boden G** 2008 Circulating FGF-21 levels in normal subjects and in newly diagnosed patients with type 2 diabetes mellitus. Exp Clin Endocrinol Diabetes 116:65–68
14. **Zhang X, Yeung DC, Karpisek M, Stejskal D, Zhou ZG, Liu F, Wong RL, Chow WS, Tso AW, Lam KS, Xu A** 2008 Serum FGF21 levels are increased in obesity and are independently associated with the metabolic syndrome in humans. Diabetes 57:1246–1253
15. **Wente W, Efanov AM, Brenner M, Kharitonenkov A, Köster A, Sandusky GE, Sewing S, Treinies I, Zitzer H, Gromada J** 2006 Fibroblast growth factor-21 improves pancreatic beta-cell function

and survival by activation of extracellular signal-regulated kinase 1/2 and Akt signaling pathways. Diabetes 55:2470–2478

16. **Ogawa Y, Kurosu H, Yamamoto M, Nandi A, Rosenblatt KP, Goetz R, Eliseenkova AV, Mohammadi M, Kuro-o M** 2007 βKlotho is required for metabolic activity of fibroblast growth factor 21. Proc Natl Acad Sci USA 104:7432–7437
17. **Kurosu H, Choi M, Ogawa Y, Dickson AS, Goetz R, Eliseenkova AV, Mohammadi M, Rosenblatt KP, Kliewer SA, Kuro-o M** 2007 Tissue-specific expression of betaKlotho and fibroblast growth factor (FGF) receptor isoforms determines metabolic activity of FGF19 and FGF21. J Biol Chem 282:26687–26695
18. **Kharitonenkov A, Dunbar JD, Bina HA, Bright S, Moyers JS, Zhang C, Ding L, Micanovic R, Mehrbod SF, Knierman MD, Hale JE, Coskun T, Shanafelt AB** 2008 FGF-21/FGF-21 receptor interaction and activation is determined by βKlotho. J Cell Physiol 215:1–7
19. **Suzuki M, Uehara Y, Motomura-Matsuzaka K, Oki J, Koyama Y, Kimura M, Asada M, Komi-Kuramochi A, Oka S, Imamura T** 2008 βKlotho is required for fibroblast growth factor (FGF) 21 signaling through FGF receptor (FGFR) 1c and FGFR3c. Mol Endocrinol 22:1006–1014
20. **Kennedy AR, Pissios P, Otu H, Xue B, Asakura K, Furukawa N, Marino FE, Liu FF, Kahn BB, Libermann TA, Maratos-Flier E** 2007 A high-fat, ketogenic diet induces a unique metabolic state in mice. Am J Physiol Endocrinol Metab [Errata (2007) 293:E1846 and (2009) 296:E1179] 292:E1724–E1739
21. **Segal-Lieberman G, Bradley RL, Kokkotou E, Carlson M, Trombly DJ, Wang X, Bates S, Myers Jr MG, Flier JS, Maratos-Flier E** 2003 Melanin-concentrating hormone is a critical mediator of the leptin-deficient phenotype. Proc Natl Acad Sci USA 100:10085–10090
22. **Kokkotou E, Jeon JY, Wang X, Marino FE, Carlson M, Trombly DJ, Maratos-Flier E** 2005 Mice with MCH ablation resist diet-induced obesity through strain-specific mechanisms. Am J Physiol Regul Integr Comp Physiol 289:R117–R124
23. **Wang H, Qiang L, Farmer SR** 2008 Identification of a domain within peroxisome proliferator-activated receptor γ regulating expression of a group of genes containing fibroblast growth factor 21 that are selectively repressed by SIRT1 in adipocytes. Mol Cell Biol 28:188–200
24. **Koester A, Broderick CL, Chen Y, Kharitonenkov A, Ford A** 2006 Metabolic evaluation of FGF-21 transgenic mice. Diabetologia 49(Suppl 1):352
25. **Shimano H, Horton JD, Hammer RE, Shimomura I, Brown MS, Goldstein JL** 1996 Overproduction of cholesterol and fatty acids causes massive liver enlargement in transgenic mice expressing truncated SREBP-1a. J Clin Invest 98:1575–1584
26. **Brown MS, Goldstein JL** 1999 A proteolytic pathway that controls the cholesterol content of membranes, cells, and blood. Proc Natl Acad Sci USA 96:11041–11048
27. **Yahagi N, Shimano H, Hasty AH, Matsuzaka T, Ide T, Yoshikawa T, Amemiya-Kudo M, Tomita S, Okazaki H, Tamura Y, Iizuka Y, Ohashi K, Osuga J, Harada K, Gotoda T, Nagai R, Ishibashi S, Yamada N** 2002 Absence of sterol regulatory element-binding protein-1 (SREBP-1) ameliorates fatty livers but not obesity or insulin resistance in Lep(ob)/Lep(ob) mice. J Biol Chem 277:19353–19357
28. **Horton JD, Shimomura I, Ikemoto S, Bashmakov Y, Hammer RE** 2003 Overexpression of sterol regulatory element-binding protein-1a in mouse adipose tissue produces adipocyte hypertrophy, increased fatty acid secretion, and fatty liver. J Biol Chem 278:36652–36660